Environmental Science & Technology

ARTICLE

pubs.acs.org/est

Hydrothermal Carbonization of Municipal Waste Streams

Nicole D. Berge,[*,†] Kyoung S. Ro,[‡] Jingdong Mao,[§] Joseph R. V. Flora,[†] Mark A. Chappell,[∥] and Sunyoung Bae[⊥]

[†]Department of Civil and Environmental Engineering, University of South Carolina, 300 Main Street, Columbia, South Carolina 29208, United States

[‡]USDA-ARS Coastal Plains Soil, Water, and Plant Research Center, 2611 West Lucas Street, Florence, South Carolina 29501, United States

[§]Department of Chemistry and Biochemistry, Old Dominion University, 4541 Hampton Boulevard, Norfolk, Virginia 23529, United States

[∥]Environmental Laboratory, U.S. Army Corps of Engineers, 3909 Halls Ferry Road, Vicksburg, Mississippi 39180, United States

[⊥]Department of Chemistry, Seoul Women's University, 139-774 126 Gongreung-Dong, Nowon-Gu, Seoul, Korea

Supporting Information

ABSTRACT: Hydrothermal carbonization (HTC) is a novel thermal conversion process that can be used to convert municipal waste streams into sterilized, value-added hydrochar. HTC has been mostly applied and studied on a limited number of feedstocks, ranging from pure substances to slightly more complex biomass such as wood, with an emphasis on nanostructure generation. There has been little work exploring the carbonization of complex waste streams or of utilizing HTC as a sustainable waste management technique. The objectives of this study were to evaluate the environmental implications associated with the carbonization of representative municipal waste streams (including gas and liquid products), to evaluate the physical, chemical, and thermal properties of the produced hydrochar, and to determine carbonization energetics associated with each waste stream. Results from batch carbonization experiments indicate 49−75% of the initially present carbon is retained within the char, while 20−37% and 2−11% of the carbon is transferred to the liquid- and gas-phases, respectively. The composition of the produced hydrochar suggests both dehydration and decarboxylation occur during carbonization, resulting in structures with high aromaticities. Process energetics suggest feedstock carbonization is exothermic.

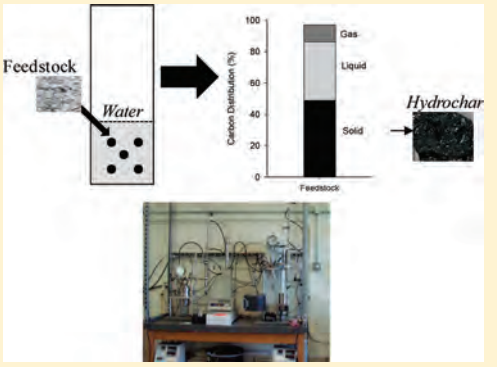

INTRODUCTION

Hydrothermal carbonization (HTC) is a novel thermal conversion process that can be a viable means for treating/stabilizing waste streams while minimizing greenhouse gas production and producing residual material with intrinsic value. HTC is a wet, relatively low temperature (180−350 °C) process that, under autogenous pressures, has been reported as a method to convert carbohydrates into a carbonaceous residue referred to as hydrochar. HTC was first experimentally explored as a means to produce coal from cellulose in 1913 by Bergius.[1,2] This process has been shown to be exothermic in nature for pure compounds[2−4] and energetically more advantageous than dry carbonization processes (e.g., pyrolysis) for feedstocks containing moisture.[1,5]

Titirici et al.[6] Sevilla and Fuertes,[7,8] and Funke and Zeigler [4] report that char formation results from a series of hydrolysis, condensation, decarboxylation, and dehydration reactions. Water is a necessary and key ingredient of HTC.[2,4] As temperatures increase, the physical and chemical properties of water change significantly, mimicking that of organic solvents.[9−11] Consequently, saturation concentrations of dissolved inorganic and organic components increase greatly and ionic reactions are promoted, ultimately enhancing hydrolysis.[4] Because hydrolysis exhibits a lower activation energy than many dry thermochemical conversion reactions, lower temperature HTC reactions can proceed with the same level of conversion efficiency as higher temperature processes.[1,4]

To date, HTC has been mostly applied and studied on a limited number of feedstocks (Table SI−S3), ranging from pure substances to slightly more complex biomass such as wood.[1] Recent motivations for utilizing this technique have concentrated on creating novel low-cost carbon-based nanomaterials/nanostructures from carbohydrates,[12,13] rather than on exploring the use of HTC as a sustainable waste management technique.[1] Results from previous studies indicate a significant fraction of carbon remains within the hydrochar during the HTC process, suggesting carbonization of waste streams may mitigate greenhouse gas emissions.[1,2,4,6−8] Reported percentages of carbon bound within

Received: February 8, 2011
Accepted: May 24, 2011
Revised: April 17, 2011
Published: June 14, 2011

dx.doi.org/10.1021/es2004528 | Environ. Sci. Technol. 2011, 45, 5696–5703

Table 1. Proximate and Ultimate Analysis of Initial Feedstocks and Produced Hydrochar[I]

	initial feedstock				hydrochar			
parameters	paper	food	mixed MSW	AD waste (dried)	paper	food	mixed MSW	AD waste
proximate analyses[a]								
moisture (%)	7.6	12.6	6.3	8.1	3.2	5.7	5.9	3.3
volatile matter ($\%_{db}$)[b]	79.6	77.6	62.0	55.9	52.8	53.4	33.6	34.5
fixed C ($\%_{db}$)	9.6	14.8	9.6	8.2	19.8	29.7	14.6	6.4
ash ($\%_{db}$)[a]	10.9	7.5	28.4	35.9	24.2	11.2	46.0	55.8
HHV (MJ/kg_{db})	14.0	18.1	16.5	15.5	23.9	29.1	20.0	13.7
ultimate analyses[c]								
H ($\%_{db}$)	5.0	5.8	3.8	4.8	4.6	5.8	2.7	3.9
C ($\%_{db}$)	36.0	42.5	28.5	32.6	57.4	67.6	33.5	27.8
O ($\%_{db}$)	48.1	40.8	38.7	20.3	12.8	9.9	14.2	7.8
N ($\%_{db}$)	0.04	3.2	0.56	5.5	0.07	4.6	0.63	2.0
S ($\%_{db}$)	0.02	0.22	0.05	0.92	0.05	0.22	0.05	0.77
av hydrochar yield ($\%_{db}$)[d]					29.2 ± 0.24	43.8 ± 3.2	63.2 ± 5.0	47.1 ± 13
av hydrochar yield ($\%_{daf}$)[e]					34.1	45.6	83.8	25.6
fixed carbon yield (%)[f]					8.5	15.8	23.9	10.6
energetic retention efficiency (%)[g]					49.8	70.3	76.8	41.5
energy densification[h]					2.2	1.82	1.73	1.5

[a] ASTM D3172. [b] ASTM D3175-07. [c] ASTM D3176-02. [d] $(M_{db,char}/M_{db,feedstock})*100$. [e] $M_{daf,char}/M_{daf,feedstock}$. [f] % char yield*(% fixed $carbon_{daf,char}$/(100-$\%ash_{feedstock}$)), as defined by ref 31. [g] $(M_{char}*HHV_{char})/(M_{feedstock}*HHV_{feedstock})$. [h] $HHV_{char}/HHV_{feedstock}$. [I] db = dry basis; daf = dry ash free basis.

the hydrochar (20−100%) vary significantly with feedstock and reaction conditions (Table SI−S3). Titirici et al.[2] report changes in feedstock composition influences degradation pathways and hydrochar's physical and chemical structure.

The potential to use the carbonized wastes (i.e., hydrochar) for environmental- and energy-related applications adds to the attractiveness of this approach. The char produced via HTC contains attractive surface functionalization patterns[2,6,8,14] that make the char amendable to beneficial end-use applications such as an adsorbent for harmful pollutants,[15] feedstock for carbon fuel cells,[16,17] and a soil amendment (similar to char from pyrolysis/gasification, e.g., ref 18). Liu et al.[15] demonstrated that hydrochar had a much higher capacity for copper removal (e.g., ion exchange) than that of char produced via pyrolysis. In addition, HTC of waste materials may require less solids processing/treatment (such as mechanical dewatering of biosolids[1,19]) and handling (hydrochar is sterilized). Carbonization may also thermally degrade or transform emerging compounds, such as pharmaceuticals, personal care products, and endocrine disrupting compounds, which currently pose significant environmental concerns/treatment challenges in waste streams.[1]

The purpose of this study was to determine the feasibility of hydrothermally carbonizing model municipal waste streams. The specific objectives of this study were to (1) evaluate the environmental implications associated with the carbonization of representative municipal waste streams (municipal solid waste and human liquid wastes), including the gas and liquid products; (2) evaluate the physical, chemical, and thermal properties of the hydrochar; and (3) determine carbonization energetics associated with each waste stream.

MATERIALS AND METHODS

Feedstocks. Model feedstocks were chosen to represent major solid and liquid waste streams. The following feedstocks were chosen for evaluation: paper (33% (wt.) of waste discarded in landfills), food waste, mixed municipal solid waste (MSW), and anaerobic digestion (AD) waste. Discarded office paper was as the paper feedstock; it was shredded (2 × 10-mm rectangles) prior to use. Rabbit food was used to simulate food wastes discarded in landfills (following ref 20) and was crushed prior to use. Mixed MSW was simulated using representative waste materials and mixed to achieve distributions typically landfilled.[21] Composition of the mixed MSW (wt. basis) is as follows: 45.5% paper (shredded discarded office paper), 9.6% glass (crushed glass bottles), 16.4% plastic (shredded discarded plastic bottles), 17.6% food (crushed rabbit food), and 10.9% metal (shredded discarded aluminum cans). AD waste (sludge) was chosen to represent human municipal waste and was acquired from an anaerobic digester at a local wastewater treatment facility. Table 1 contains the physical and chemical characteristics associated with these feedstocks.

Carbonization Experiments. HTC of the waste streams was conducted in 160-mL stainless steel tubular reactors rated to withstand anticipated temperatures and pressures. Carbonization of the feedstocks was conducted by loading each reactor with dry solids and DI water to obtain a solids concentration of 20% (wt.). The AD waste was received as a wet waste stream, consisting of approximately 3.0% (wt.) solids. The total mass of AD waste added to each reactor was equivalent to the total mass of that added to reactors containing the dry feedstock. All reactors were heated to 250 °C in a laboratory oven for 20 h. The reactors were removed from the oven and subsequently placed in a cold water bath to quench the reaction. After the reactors were cooled, samples from the solid (proximate and ultimate analysis, energy content, ^{13}C solid-state NMR), liquid (total organic carbon (TOC), pH, chemical oxygen demand (COD), biochemical oxygen demand (BOD)), and gas phases (gas volume and carbon dioxide) were taken to allow determination of carbon distribution, process energetics, process water quality, and gas

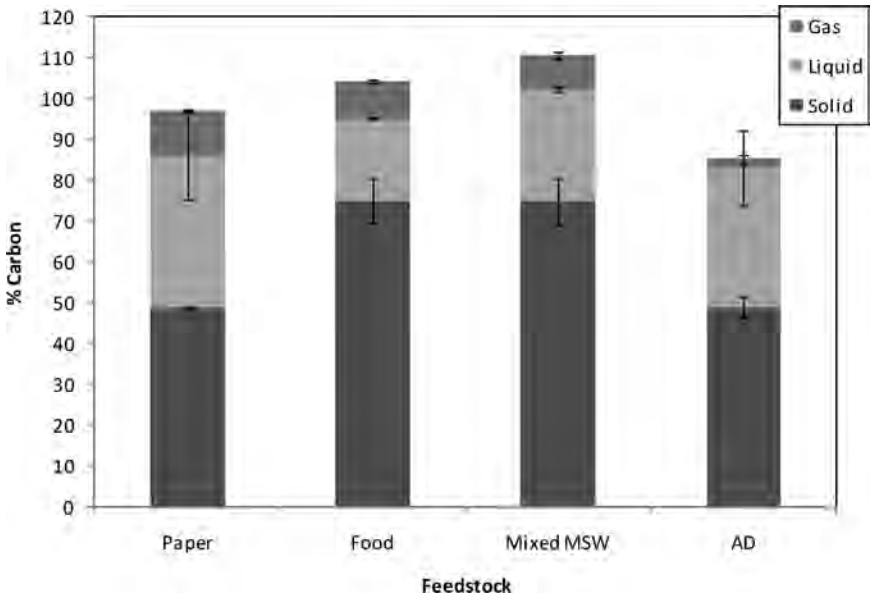

Figure 1. Distribution of carbon following the hydrothermal carbonization of each feedstock. Values represent averages from triplicate analyses. Error bars represent standard deviations.

composition. Details regarding specific analytical techniques are available in the Supporting Information.

RESULTS AND DISCUSSION

Carbon Distribution. The carbon content of the produced hydrochars ranges from 28−68% (Table 1). Carbon contents of hydrochars resulting from the carbonization of other compounds were reported in the literature range from 20−78% (Table SI−S3). It is difficult, however, to make direct comparisons between hydrochar carbon contents reported in the literature and those measured in this study, as temperature, pressure, reaction time, reactor design, and solids concentration influence carbonization extent. It should be noted that carbonization conditions (e.g., temperature and time) for the waste streams were not optimized in this study.

Mass balance analyses indicate that carbonization of the feedstocks results in a significant fraction of carbon retained within the char (Figure 1). Carbonization of office paper and AD waste results in the smallest fraction of carbon remaining in the solid-phase (Figure 1). The carbon sequestered during HTC of office paper is greater than that currently achieved when landfilling the paper. Barlaz[22] developed carbon storage factors (CSFs, mass of carbon remaining in the solid following biological decomposition in a landfill/dry mass of feedstock) as a means to compare the mass of carbon remaining (stored) within solid material following biological decomposition in landfills. The reported CSF associated with office paper in landfills is 0.05. The estimated CSF from hydrothermally carbonized office paper is 0.18 (see the Supporting Information), indicating more carbon remains stored within the solid material following HTC than if the paper had been landfilled. This provides evidence suggesting that HTC may be a promising process for mitigating carbon emissions associated with management of waste paper. The reported CSFs for food waste and mixed MSW in landfills reported by Barlaz[22] are 0.08 and 0.22, respectively. A CSF of 0.34 and 0.23 for food and mixed MSW, respectively, results from the HTC of the wastes (Table SI−S1). Although comparing the CSFs reported by Barlaz[22] and those from HTC are useful in contrasting the fate of carbon resulting from each treatment technique, global implications from this analysis should be used with caution, as long-term stability of carbon in the char is not well understood.

The carbon content of the AD waste is slightly smaller than the initial feedstock following carbonization, suggesting the carbonization of AD waste may not be effective. Prior to carbonization, the AD waste has undergone significant stabilization and is slightly basic. Carbonization of stabilized solids may have little impact on carbon fate, as suggested by the small change in carbon content of the initial and carbonized AD waste.

Smaller fractions of the carbon are transferred to either the gas- or liquid-phases, as illustrated in Figure 1. The gas produced in each system is small and accounts for approximately 2−11% of the carbon. The gas is predominantly carbon dioxide, with trace amounts of other gases (Figure SI−S1). The total organic carbon of the liquid extracts was measured and used to compute the fraction of initially present carbon found in the liquid. Results indicate approximately 20−37% of the carbon is transferred to the liquid-phase. The composition of both the liquid- and gas-phases will be discussed in subsequent sections. Carbon recoveries ranged from 81−115% (Figure 1). Similarly to that described by Funke and Ziegler[4] and Karagoz et al.[23] an immiscible liquid-phase was also observed. It is likely unrecovered carbon exists in this fraction.

Process Water Composition. Several organic compounds were detected in the HTC process water. Acetic acid is present in all samples and is likely a product of the decomposition of hydrolysis products.[7,8,24] Several aromatics, aldehydes, and alkenes were also detected (Table SI−S4). Additionally, furanic and phenolic compounds (similar to those reported by Sevilla and Fuertes[7,8]) were identified, suggesting the pathway of carbonization follows those previously reported: hydrolysis, dehydration, decarboxylation, condensation, and decomposition of the various intermediates. Leaching tests (see the Supporting Information for details) confirm the compounds identified in the

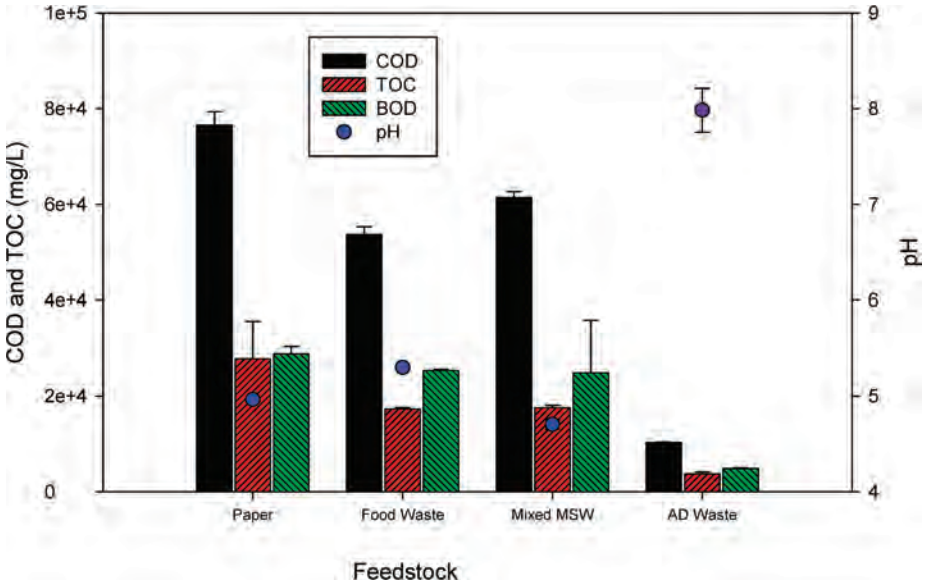

Figure 2. HTC process water quality. Values are based on the average from triplicate reactors. Error bars represent the standard deviation.

process water are due to thermal degradation of the feedstock. The COD, BOD, and TOC concentrations of the HTC process water (Figure 2) are equivalent to those typically found in landfill leachate.[25] The pH of all process waters, except that of the AD waste, was acidic, likely due to the presence of organic acids resulting from the decomposition of monosacharides.[7,8] The pH of the AD process water remained slightly basic (due to high buffering capacity of the AD water) which may have hindered the initial hydrolysis step of the carbonization process. When evaluating the hydrochar yield on an ash-free basis (Table 1), the AD waste resulted in a lower char yield than the other feedstocks.

Management of this process water needs to be considered. The BOD/COD ratio of the waters was >0.3, suggesting it is amenable to subsequent biological treatment. Funke and Zeigler[3] report the liquid can be effectively treated via common aerobic processes. It may be possible to recover some of the chemicals from the water for use/reuse. Alternatively, it may be possible to recycle the process water, using it as the liquid source for subsequent carbonization.

Gas Composition. Gas composition resulting from carbonization of feedstocks has not been well-explored or well-reported. The purpose of this analysis was to identify gases being produced during HTC to determine potential environmental impacts and/or any energy significance. The gas produced as a result of carbonization is small (2−11% of total carbon, Figure 1). The major component of the gas is carbon dioxide, indicating decarboxylation occurs (Figure SI−S1). Several trace gases were also identified (Figure SI−S1). Results suggest gas composition does not vary significantly with feedstock. Several of the trace compounds detected may be utilized for subsequent energy generation (e.g., methane, hydrogen). Of environmental concern is the detection of furans. Furan production likely results from the thermal decomposition of the cellulosic materials, condensation of aromatic compounds, and/or the thermal oxidation of lipids.[26−28] Furans are currently emitted from waste and landfill gas combustion (e.g., refs 29 and 30). The smallest volume of gas was produced when carbonizing the AD waste. This gas stream also contains the lowest concentrations of the trace compounds. This observation is consistent with the insignificant change in AD solid-phase carbon, likely a result of incomplete initial hydrolysis.

Char Characteristics. *Physical Characteristics.* Hydrochar yields ranged from 29−63% (Table 1). The smallest hydrochar yield is that associated with the carbonization of paper (29.2%). The largest yield is obtained from the carbonization of MSW; however, this yield is skewed because of the recovery of the inert, unmodified components of MSW (e.g., glass and metal). The yields observed in these experiments fit within the reported range of hydrochar yields associated with various feedstocks (Table SI−S3). Although some metals have been shown to have a catalytic effect on carbonization (e.g., silver, iron oxides[2,6]), the metal component of the mixed MSW waste (aluminum) does not appear to influence solid yield, as the hydrochar yield associated with mixed MSW can be derived using the yields associated with paper and food.

As expected, the mass of volatile carbon in the solid decreased significantly (approximately 64−79% reduction, see the Supporting Information) as a result of carbonization. The fixed carbon yields resulting from carbonization range from 8.5−24% (Table 1) and represent the efficiency of the hydrothermal conversion of ash-free organic matter in the feedstock to ash-free carbon (as defined by ref 31). These values are significantly lower than those reported for the pyrolysis of wood (ranges from 28−33%, ref 31). Also, the fixed carbon content of the hydrochars is lower than those resulting from the hydrothermal carbonization of other feedstocks. Liu et al.[15] reported a fixed carbon content of carbonized pinewood to be 43%. The fixed carbon yield is greatly influenced by process conditions. As indicated previously, carbonization conditions have not been optimized for these waste streams. Larger fixed carbon yields may result at different temperatures, reaction times, and/or solids concentrations.

Chemical Characteristics. The elemental composition of the solid material changes significantly as a result of carbonization (Table 1). H/C and O/C atomic ratios were computed for the initial feedstock and the resulting hydrochar and were analyzed using a Van Krevelen diagram (Figure 3). Van Krevelen diagrams allow for delineation of reaction pathways. Straight lines can be drawn to represent the dehydration and decarboxlation reaction pathways. As illustrated in Figure 3, the conversion of food, paper, and mixed MSW is predominantly governed by the dehydration

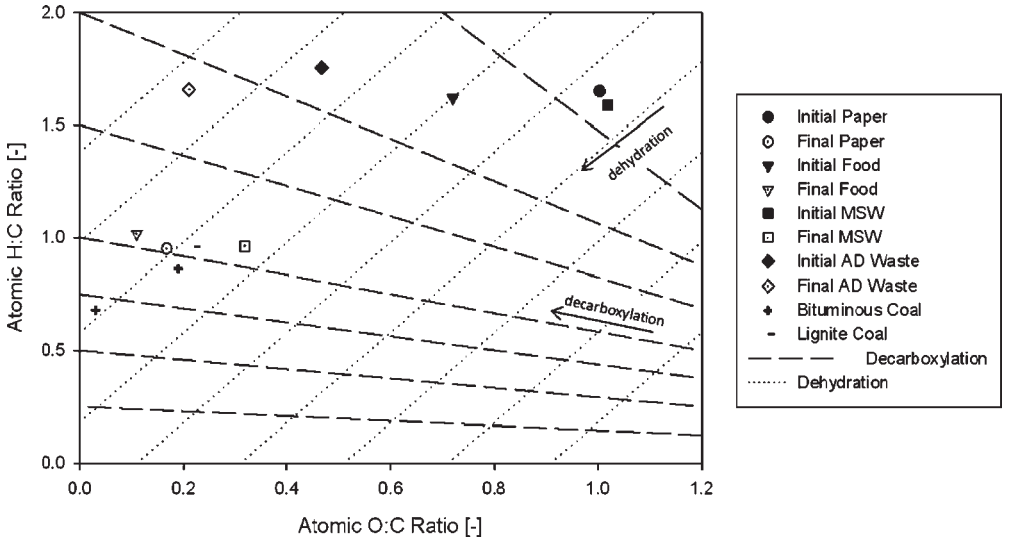

Figure 3. Atomic H/C and O/C ratios of the feedstocks and chars resulting from carbonization. The atomic ratios for bituminous (two data points representing a range of H/C and O/C ratios) and lignite coals are included for comparative purposes. The lines represent dehydration and decarboxylation pathways.

process (lower H/C). A shift in the O/C ratio suggests that decarboxylation also occurs. This is similar to that observed for the hydrothermal carbonization of glucose, cellulose, sucrose, and starch.[7,8] The conversion of AD waste, however, appears to be largely influenced by decarboxylation (Figure 3). The difference in reaction mechanism is likely due to the alkaline conditions of the AD waste. The pH of feedstock has been reported as a parameter that has significant impact on reaction mechanisms.[1,4,6] The pH of the AD process water is 8, while that associated with the other feedstocks is ~5.0. Alkaline conditions often are used during liquefaction of biomass and result in a char with a high H/C ratio.[1] The atomic ratios of the hydrochars (except that associated with AD waste) are similar to those associated with bituminous and lignite coals (Figure 3).

Another important characteristic of the hydrochars is the high higher heating value (HHV) (Table 1). The HHVs correlate well with carbon content of the organic solids (Figure SI−S2). These results are similar to a relationship previously reported by Ramke et al.[32] Using a relationship developed by Ramke et al.[32] for carbonized organic waste streams (e.g., grass, wood), the HHVs of the paper and food waste can be predicted with <11% error (Table SI−S6). The inorganic components of the MSW feedstock limit the applicability of this relationship (Figure SI−S2). Using results from the ultimate analysis of the hydrochars (Table 1), the HHVs of all chars, except that resulting from the carbonization of the MSW, can also be accurately predicted with the relationship described by Channiwala and Parikh.[33] Because solid mass decreases due to dehydration and decarboxylation reactions, energy densification occurs. The energy densification factors associated with the hydrochars from the waste materials evaluated range from 1.5−2.2 (Table 1). Energetic retention efficiencies (defined by ref 3) provide a means for comparing the energy remaining within the char and range from 42% (for AD waste) to 76% (MSW) (Table 1).

NMR Results. Figure SI−S3 shows the spectra of ^{13}C CP/TOSS and ^{13}C CP/TOSS with 40-μs dipolar dephasing of feedstocks and their respective HTC chars. ^{13}C CP/TOSS spectra provide semiquantitative whole structural information and dipolar-dephased spectra select signals of nonprotonated carbons and carbons of mobile groups such as CCH_3 groups.

The ^{13}C CP/TOSS spectrum of food waste (Figure SI−S3(a)) indicates it is primarily composed of (1) carbohydrates, (2) proteins/peptides, and (3) lipids. Signals from lipids and proteins are very small compared with those of carbohydrates. The ^{13}C CP/TOSS spectrum of paper shows exclusively the signals of carbohydrates (cellulose) (Figure SI−S3(e)). The NMR spectra of mixed MSW was not acquired because it is basically the stacking of the ^{13}C CP/TOSS spectra of food, paper, and polyethylene terephthalate (PET) in the proper proportions (45.5% paper, 16.4% plastic, and 17.6% food). The chemical structure of the AD waste (Figure SI−S3(k)) is relatively complex compared with that of food and paper. Based on the NMR results, AD waste contains significant (1) proteins or peptides, (2) long-chain -$(CH_2)_n$- of lipids, and (3) carbohydrates. The semiquantitative structural information of each feedstock is displayed in Table 2. More specific details regarding the analysis of the feedstock NMR spectra can be found in the Supporting Information.

The characteristics of the produced chars are significantly different than their respective feedstocks. The ^{13}C CP/TOSS spectrum of food char is primarily composed of two broad bands representing sp^3-hybridized carbons (0−92 ppm) and sp^2-hybridized carbons (92−220 ppm), resembling the spectra of geological samples such as kerogen and coal.[34,35] The spectrum shows CCH_3 signals at 13 ppm (methyl end chain ω), 22 ppm (methylene carbons next to the methyl end carbons, ω-1), 31 ppm (mobile methylene carbons, ω-2), and 172 ppm (COO), indicating the presence of lipids.[36,37] Most of the aromatics are nonprotonated, since the aromatic signals around 128 ppm dephase little in the dipolar-dephased spectrum (Figure SI−S3(d)). This suggests the char is composed of fused ring aromatics, which are highly bioresistant and may contribute to the long-term stability of the hydrochar. The dipolar dephasing spectrum also indicates that the signals around 200 ppm are all attributed to ketones.

The characteristics of ^{13}C CP/TOSS spectrum of paper HTC char differ from that of food char. Its aliphatic signals are broad,

Table 2. Semiquantitative Information of Functional Groups

	ppm						
sample	190−220 carbonyl	165−190 COO/N−C═O	165−145 aromatic C−O	112−145 aromatic/olefinic C	112−60 O-alkyl C	60−48 NCH/OCH_3	48−0 alkyl
initial food	0.3	5.2	1.3	3.1	69.0	7.9	13.3
HTC food	2.1	3.9	7.4	34.1	6.8	3.5	42.3
initial paper	0.0	0.3	0.1	0.4	95.7	2.9	0.6
HTC paper	3.3	4.2	7.2	29.1	8.0	6.4	41.8
HTC msw mixed	3.1	8.1	7.4	39.5	7.6	4.2	30.2
initial anaerobic digestion waste	1.6	15.5	2.0	8.5	25.9	10.5	36.1
HTC anaerobic digestion waste	0.9	3.1	4.9	29.1	9.6	3.3	49.2

Table 3. Heat of Reactions Associated with the Carbonization of Each Feedstock at 250 °C

reactions[a]	heat of reaction (MJ/kg feedstock)[b]
paper → char + dissolved organics + CO_2	−0.68
$CH_{1.67}ON_{0.001}S_{0.0002} \rightarrow 0.46\ CH_{0.96}O_{0.168}N_{0.001}S_{0.0003} + 0.54\ CH_{2.3}O_{1.71}N_{0.0009}S_{0.0001} + 5.5 \times 10^{-6}\ CO_2$	
food → char + dissolved organics + CO_2	−1.19
$CH_{1.63}O_{0.72}N_{0.064}S_{0.002} \rightarrow 0.7\ CH_{1.03}O_{0.11}N_{0.06}S_{0.001} + 0.30\ CH_3O_{2.11}N_{0.075}S_{0.0036} + 5.14 \times 10^{-6}\ CO_2$	
mixed MSW → char + dissolved organics + CO_2	−2.62
$CH_{1.60}O_{1.02}N_{0.017}S_{0.0007} \rightarrow 0.74\ CH_{0.97}O_{0.32}N_{0.016}S_{0.0006} + 0.26\ CH_{3.4}O_{3.06}N_{0.019}S_{0.0009} + 6.6 \times 10^{-6}\ CO_2$	
AD waste → char + dissolved organics + CO_2	−0.75
$CH_{1.77}O_{0.47}N_{0.14}S_{0.01} \rightarrow 0.40\ CH_{1.67}O_{0.21}N_{0.063}S_{0.01} + 0.60\ CH_{1.8}O_{0.64}N_{0.20}S_{0.011} + 6.5 \times 10^{-6}\ CO_2$	
cellulose[c] → char + CO_2 + water	−1.6
$C_6H_{12}O_5 \rightarrow C_{5.25}H_4O_{0.5} + 0.75\ CO_2 + 3\ H_2O$	

[a] All reactions occurred at 250 °C for 20 h, with an initial solids concentration of approximately 20% (wt.), except for the AD waste. [b] Values were determined based on feedstock and char measured HHV and combustion reactions. The composition of dissolved organics found in the liquid was determined using mass balances. The HHV of the dissolved organics in the liquid was estimated using the relationship provided by ref 33. Trace gas production was neglected. [c] Taken from ref 1.

with more intensities below and above 31 ppm (CCHC and CCH_3). In contrast, the aliphatic region of ^{13}C CP/TOSS spectrum of food char is dominated by a sharp $C(CH_2)_nC$ band at 31 ppm. Its aromatic signals are characterized by one band around 128 ppm with two shoulders around 142 ppm and 150 ppm, respectively. The shoulder around 150 ppm is attributed to aromatic C−O groups. In addition, there is a distinct band around 170 ppm attributed to COO/N−C═O and another around 208 ppm due to ketones or aldehydes. The dipolar-dephased spectrum shows signals of mobile CCH_3 groups around 13 ppm, a small but broad band ranging from 40 to 70 ppm, likely attributed to nonprotonated oxygen-containing functional groups. The dipolar-dephased spectrum clearly reveals that its aromatic band around 128 ppm is attributed to protonated aromatics whereas the aromatic signals around 142 ppm are due to nonprotonated ones (Figure SI−S3(h)). In addition, the signals around 208 ppm are attributed to ketones since they survive after dipolar dephasing.

The ^{13}C CP/TOSS spectrum of mixed MSW HTC char, Figure SI−S3(i), indicates that HTC processes cannot degrade PET (physical alteration may occur), as demonstrated by the presence of the distinct sharp PET signals. The dipolar-dephased spectrum show CCH_3 signals at 13 ppm with one shoulder at 22 ppm and small CCH_2C signals around 31 ppm. The dipolar-dephased spectrum also shows that nonprotonated aromatic band of PET around 130 ppm is stacked on the top of broad nonprotnated aromatics from MSW char; similarly the sharp COO signal from PET at 164.3 ppm is stacked on the broad COO band from MSW char. A shoulder around 150 ppm is assigned to aromatic C−O groups and the band around 208 ppm attributed to ketones (Figure SI−S3(j)).

The ^{13}C CP/TOSS spectrum of the HTC char from the AD waste consists primarily of two dominant bands of aliphatics and aromatics around 30 ppm and 128 ppm, respectively, which seems to be similar to that of food HTC char (Figure SI−S3(c)). However, their dipolar-dephased spectra are significantly different (Figures SI−S3(d) and (n)), with much more mobile -$(CH2)_n$- in AD waste HTC char. Small, broad signals between 165 and 190 ppm are due to COO/N−C═O and those between 190 and 210 ppm are assigned to aldehydes or ketones. The band between 60 and 90 ppm is retained in the dipolar dephasing spectrum (Figure SI−S3(n)), indicating that they are nonprotonated O-alkyls. Dipolar dephasing also reveals that most of aromatics are nonprotonated, likely contributing to the long-term stability of the hydrochar. We do not observe signals above 190 ppm in the dipolar-dephased spectrum, indicating that the signals around this region are all attributed to protonated aldehydes. Furthermore, the dipolar-dephased spectrum also indicates that most of the nonpolar alkyls, $C(CH_2)_nC$ and CCH_3 groups, are mobile.

The semiquantitative structural information of the HTC chars are displayed in Table 2 which also indicates the composition of the chars varies significantly from that of the feedstocks. These results confirm that both decarboxylation (disappearance of the

COO band) and dehydration (increase of nonprotonated aromatics) occur (as suggested in the Van Krevelen diagram). HTC chars are dominated by alkyls (30.2% to 49.2%) and aromatics (29.1% to 39.5%). Except for the mixed MSW char, alkyls are the largest component of the chars and aromatics the second. Note that mixed MSW char is a mixture of char and nondegraded PET. The O-alkyl groups present in the initial solids, attributed primarily to carbohydrates, are significantly smaller in the HTC chars, suggesting carbohydrates were degraded. Increases in the aromatic fraction in the solids suggest condensation polymerization occurs during carbonization.[36] Except for the mixed MSW char, the food char has the highest aromaticity (aromatics + aromatic C−O), whereas char from the AD waste has the lowest. The decrease in the COO/N−C═O groups in the char from the carbonization of food and AD waste suggests the hydrolysis of proteins occurred, similar to that observed during the HTC of swine waste.[36]

Process Energetics. HTC reactions are difficult to construct because of the numerous intermediates detected in the gas and liquid-phases. Process reactions have thus been commonly simplified by neglecting liquid and gaseous (other than CO_2) products.[1,2,4] The liquid intermediates, however, represent a significant fraction of products (20−37% of initially present carbon) and likely have an important impact on process energetics.

Carbonization energetics associated with the feedstocks evaluated in this study were determined by constructing simplified HTC reactions (Table 3) based on feedstock and char elemental composition (Table 1), measured carbon dioxide production, and simplified composition of organics in the liquid- and gas-phases. The composition of dissolved organics was determined using mass balances (C, H, O, N, and S present in the feestock that were not found in the char or gas were assumed to be in the liquid). The gas-phase carbon in the constructed reactions is represented by carbon dioxide, as it was the predominant gas measured; other trace organic gases produced (Figure SI−S1) were neglected. Nitrogen and sulfur fate were not individually tracked during these experiments, and thus it was assumed all nitrogen and sulfur not present in the hydrochar remains within the liquid-phase.

Heat of formations associated with the feedstock and hydrochar were estimated based on measured HHVs and combustion reactions. The HHV of the dissolved organics in the liquid was estimated using the unified correlation for estimating HHV from solid, liquid, and gaseous fuels provided by Channiwala and Parikh.[33] Heats of reaction were then calculated. Results are presented in Table 3 and suggest HTC is exothermic for each feedstock. The values compare well to those reported for the HTC of cellulose (neglecting liquid intermediates). Libra et al.[1] report a heat of reaction of cellulose to be -1.6 MJ/$kg_{cellulose}$.

The energy required to heat the water to the reaction temperature (250 °C) must also be considered in an energetic analysis of HTC. Because, during HTC, the phase change from water to steam is largely avoided, the required energy to heat the water (in a closed system to saturation conditions) is small in comparison to that required to evaporate water in traditional, dry thermochemical conversion processes. The energy required to heat the water (with 20% solids) from 25 to 250 °C in 160-mL closed reactors is 4.5 MJ/$kg_{feedstock}$ (see the Supporting Information). In comparison, the energy required to evaporate the same volume of water is approximately 2.4 times larger (10.3 MJ/$kg_{feedstock}$, assuming 20% solids).

■ ASSOCIATED CONTENT

Supporting Information. Details of methods, feedstock NMR spectral analysis, CSF calculations, calculations describing the volatile carbon decrease as a result of HTC, selected studies investigating hydrothermal carbonization of various feedstocks, gas composition, compounds identified in the process water and leachant solutions, results from leaching study, process water quality, the relationship between HHV and hydrochar carbon content, and calculations of energy to evaporate/heat water. This material is available free of charge via the Internet at http://pubs.acs.org.

■ AUTHOR INFORMATION

Corresponding Author

*Phone: (803) 777-7521. Fax: (803) 777-0670. E-mail: berge@cec.sc.edu.

■ ACKNOWLEDGMENT

The authors acknowledge the contributions of Ms. Beth Quattlebaum for conducting AD waste experiments and Ms. Paula Lozano for obtaining TOC data. Mao would like to thank the National Science Foundation (EAR-0843996 and CBET-0853950) for the support of his research. Collaboration with the USDA-ARS was conducted according to the agreement NFCA 6657-13630-003-14N. Mention of trade names or commercial products is solely for the purpose of providing specific information and does not imply recommendation or endorsement by the U.S. Department of Agriculture.

■ REFERENCES

(1) Libra, J.; Ro, K.; Kammann, C.; Funke, A.; Berge, N.; Neubauer, Y.; Titirici, M.; Fuhner, C.; Bens, O.; Emmerich, K. Hydrothermal carbonization of biomass residuals: a comparative review of the chemistry, processes and applications of wet and dry pyrolysis. *Biofuels* **2011**, *2* (1), 89–124.

(2) Titirici, M. M.; Thomas, A.; Antonietti, M. Back in the black: hydrothermal carbonization of plant material as an efficient chemical process to treat the CO2 problem? *New J. Chem.* **2007**, *31*, 787–789.

(3) Funke, A.; Ziegler, F., Hydrothermal carbonization of biomass: A literature survey focusing on its technical application and prospects. In *17th European Biomass Conference and Exhibition*, Hamburg, Germany, 2009; pp 1037−1050.

(4) Funke, A.; Ziegler, F. Hydrothermal carbonization of biomass: A summary and discussion of chemical mechanisms for process engineering. *Biofuels, Bioprod. Biorefin.* **2010**, *4* (2), 160–177.

(5) Erlach, B.; Tsatsaronis, G. In *Upgrading of biomass by hydrothermal carbonisation:analysis of an industrial-scale plant design*, ECOS 2010- 23rd International Conference on Efficiency, Cost, Optimization, Simulation and Environmental Impact of Energy Systems, 2010; 2010.

(6) Titirici, M. M.; Thomas, A.; Yu, S. H.; Muller, J. O.; Antonietti, M. A direct synthesis of mesoporous carbons with bicontinuous pore morphology from crude plant material by hydrothermal carbonization. *Chem. Mater.* **2007**, *19* (17), 4205–4212.

(7) Sevilla, M.; Fuertes, A. B. The production of carbon materials by hydrothermal carbonization of cellulose. *Carbon* **2009**, *47* (9), 2281–2289.

(8) Sevilla, M.; Fuertes, A. B. Chemical and structural properties of carbonaceous products obtained by hydrothermal carbonizatioon of saccharides. *Chem.—Eur. J.* **2009**, *15*, 4195–4203.

(9) Akiya, N.; Savage, P. E. Roles of water for chemical reactions in high-temperature water. *Chem. Rev.* **2002**, *102* (8), 2725–2750.

(10) Siskin, M.; Katritzky, A. R. Reactivity of organic compounds in superheated water: General background. *Chem. Rev.* **2001**, *101* (4), 825–835.

(11) Wantanabe, M.; Sato, T.; Inomata, H.; Smith, R.; Arai, K.; Kruse, A.; Dinjus, E. Chemical reactions of C1 compounds in near-critical and supercritical water. *Chem. Rev* **2004**, *104*, 5803–5821.

(12) White, R. J.; Budarin, V.; Luque, R.; Clark, J. H.; Macquarrie, D. J. Tuneable porous carbonaceous materials from renewable resources. *Chem. Soc. Rev.* **2009**, *38*, 3401–3418.

(13) Yu, S.; Cui, X.; Li, L.; Li, K.; Yu, B.; Antonietti, M.; Colfen, H. From starch to metal/carbon hybrid nanostructures: hydrothermal metal-catalyzed carbonization. *Adv. Mater.* **2004**, *18*, 1636–1640.

(14) Titirici, M.; Antonietti, M. Chemistry and materials options of sustaibale carbon materials made by hudrothermal carbonization. *Chem. Soc. Rev.* **2010**, *39*, 103–116.

(15) Liu, Z.; Zhang, F.-S.; Wu, J. Characterization and application of chars produced from pinewood pyrolysis and hydrothermal treatment. *Fuel* **2010**, *89*, 510–514.

(16) Cao, S.; Sun, Y.; Wang, G. Direct carbon fuel cell: Fundamentals and recent developments. *J. Power Sources* **2007**, *167* (2), 250–257.

(17) Paraknowitsch, J. P.; Thomas, A.; Antonietti, M. Carbon Colloids Prepared by Hydrothermal Carbonization as Efficient Fuel for Indirect Carbon Fuel Cells. *Chem. Mater.* **2009**, *21* (7), 1170–+.

(18) Spokas, K. A.; Reicosky, D. C. Impacts of sixtenn different biochars on soil greenhouse gas production. *Ann. Environ. Sci.* **2009**, *3*, 179–193.

(19) Mursito, A. T.; Hirajima, T.; Sasaki, K., Upgrading and dewatering of raw tropical peat by hydrothermal treatment. *Fuel 89*, (3), 635-641.

(20) Wu, B. Y.; Taylor, C. M.; Knappe, D. R. U.; Nanny, M. A.; Barlaz, M. A. Factors controlling alkylbenzene sorption to municipal solid waste. *Environ. Sci. Technol.* **2001**, *35* (22), 4569–4576.

(21) USEPA, Municipal Solid Waste in the United States: 2005 Facts and Figures. 2006.

(22) Barlaz, M. A. Carbon storage during biodegradation of municipal solid waste components in laboratory-scale landfills. *Global Biochemical Cycles* **1998**, *12* (2), 373–380.

(23) Karagoz, S.; Bhaskar, T.; Muto, A.; Sakata, Y.; Oshiki, T.; Kishimoto, T. Low-temperature catalytic hydrothermal treatment of wood biomass: analysis of liquid products. *Chem. Eng. J.* **2005**, *108* (1−2), 127–137.

(24) Goto, M.; Obuchi, R.; Hiroshi, T.; Sakaki, T.; Shibata, M. Hydrothermal conversion of municipal organic waste into resources. *Bioresour. Technol.* **2004**, *93* (3), 279–284.

(25) Kjeldsen, P.; Barlaz, M. A.; Rooker, A. P.; Baun, A.; Ledin, A.; Christensen, T. H. Present and long-term composition of MSW landfill leachate: A review. *Crit. Rev. Environ. Sci. Technol.* **2002**, *32* (4), 297–336.

(26) Ball, R.; McIntosh, A. C.; Brindley, J. The role of char-forming process in the thermal decomposition of cellulose. *Phys. Chem. Chem. Phys.* **1999**, *1*, 5035–5043.

(27) Perez Locas, C.; Yaylayan, V. A. Origin and Mechanistic Pathways of Formation of the Parent FuranA Food Toxicant. *J. Agric. Food Chem.* **2004**, *52* (22), 6830–6836.

(28) Russell, J. A.; Miller, R. K.; Molton, P. M. Formation of aromatic compounds from condensation reactions of cellulose degradation products. *Biomass* **1983**, *3* (1), 43–57.

(29) Brosseau, J.; Heitz, M. Trace gas compound emissions from municipal landfill sanitary sites. *Atmos. Environ.* **1994**, *28* (2), 285–293.

(30) Williams, P. T. Dioxins and furans from the incineration of municipal solid waste: an overview. *J. Energy Inst.* **2005**, *78* (1), 38–46.

(31) Antal, M. J.; Gronli, M. The art, science, and technology of charcoal production. *Ind. Eng. Chem. Res.* **2003**, *42* (8), 1619–1640.

(32) Ramke, H. G.; Blohse, D.; Lehmann, H. J.; Fettig, J. In *Hydrothermal carbonization of organic waste*, Twelfth International Waste Management and Landfill Symposium, Sardinia, Italy, 2009; Sardinia, Italy, 2009.

(33) Channiwala, S. A.; Parikh, P. P. A unified correlation for estimating HHV of solid, liquid and gaseous fuel. *Fuel* **2002**, *81*, 1051–1063.

(34) Mao, J.-D.; Fang, X.; Lan, Y.; Schimmelmann, A.; Mastalerz, M.; Xu, L.; Schmidt-Rohr, K. Chemical and nanometer-scale structures of kerogen and their changes during thermal maturation investigated by advanced solid-state NMR spectroscopy. *Geochim. Cosmochim. Acta* **2010**, *74*, 2110–2127.

(35) Mao, J.-D.; Schimmelmann, A.; Mastalerz, M.; Hatcher, P. G.; Li, Y. Structural features of a bituminous coal and their changes during low-temperature oxidation and loss of volatiles investigated by advanced solid-state NMR spectroscopy. *Energy Fuels* **2010**, *24*, 2536–2544.

(36) Cao, X.; Ro, K. S.; Chappell, M.; Li, Y.; Mao, J.-D. Chemical structures of swine-manure chars produced under different carbonization conditions investigated by advanced solid-state ^{13}C NMR spectroscopy. *Energy Fuels* **2011**, *25*, 388–397.

(37) Mao, J.-D.; Ajakaiye, A.; Lan, Y.; Olk, D. C.; Ceballos, M.; Zhang, T.; Fan, M. Z.; Forsberg, C. W. Chemical structures of manure from conventional and phytase transgenic pigs investigated by advanced solid-state NMR spectroscopy. *J. Agric. Food Chem.* **2008**, *56*, 2131–2138.